Reprinted from JOURNAL OF STATISTICAL PHYSICS

Vol. 70, Nos. 1/2, January 1993
Printed in Belgium

Spectral Characteristics and Synchrony in Primary Auditory-Nerve Fibers in Response to Pure-Tone Acoustic Stimuli

Malvin C. Teich,[1] Shyam M. Khanna,[2] and Patrick C. Guiney[3]

Under pure-tone stimulation, the spectrum of the period histogram recorded from primary auditory-nerve fibers at low and medium frequencies contains components at DC, at the applied tone frequency (the fundamental), and at a small number of harmonics of the tone frequency. The magnitudes and phases of these spectral components are examined. The spectral magnitudes of the fundamental and various harmonic components generally bear a fixed proportionality to each other over a broad range of signal conditions and nerve-fiber characteristics. This implies that the shape of the underlying rectified wave remains essentially unchanged over a broad range of stimulus intensities. For high-frequency stimuli, the fundamental and harmonic components are substantially attenuated. We provide a theoretical basis for the decrease of the spectral-component magnitudes with increasing harmonic number. For low-frequency pure-tone signals, the decrease is caused principally by the uncertainty in the position of neural-event occurrences within the half-wave-rectified period histogram. The lower the stimulus frequency, the greater this time uncertainty and therefore the lower the frequency at which the spectral components begin to diminish. For high-frequency pure-tone signals, on the other hand, the decrease is caused principally by the frequency rolloff associated with nerve-spike time jitter (it is then called loss of phase locking or loss of synchrony). Since some of this jitter arises from noise in the auditory nerve, it can be minimized by using peak detection rather than level detection. Using a specially designed microcomputer that measures the times at which the peaks of the action potentials occur, we have demonstrated the presence of phase locking to

[1] Departments of Electrical Engineering and Applied Physics, Columbia University, New York, New York 10027.
[2] Fowler Memorial Laboratory, Department of Otolaryngology, Columbia College of Physicians & Surgeons, New York, New York 10032.
[3] Department of Electrical Engineering, Columbia University, New York, New York 10027.

0022-4715/93/0100-0257$07.00/0

tone frequencies as high as 18 kHz. The traditional view that phase locking is always lost above 6 kHz is clearly not valid. This indicates that the place-versus-periodicity dichotomy in auditory theory requires reexamination.

KEY WORDS: Stochastic point process; auditory-nerve fibers; pure tones; neural coding; spectral characteristics; synchrony.

1. INTRODUCTION

The manner in which acoustic information is encoded into the parallel sequences of action potentials on the auditory nerve continues to perplex us, even though some 50 years have passed since the first auditory neural-spike measurements were made. In an attempt to unravel the coding mechanisms, the neural responses of mammalian primary auditory-nerve fibers have been studied extensively.[5–7,13,17,19,20,27,30,31,33,34,36,42] Many of these studies have made use of pure-tone stimuli and the period histogram, which provides a method for examining the average behavior of ensembles of nerve impulses in the time domain.[8,12,20,29] The responses of these cells are stochastic and a broad range of statistical models has been invoked to explain them. These range from simple renewal models[20] to stochastic resonance[25] to doubly stochastic Poisson point processes driven by fractal shot noise.[26,34,35,41]

The mechanisms of information encoding can be elucidated by examining the spectral components of the period histogram, obtained by means of the discrete Fourier transform (DFT).[1,23] It is well known that certain spectral components emerge when the stimulus is a pure tone at a sufficiently low frequency: these include components at DC, at the applied tone frequency, and at a small number of harmonics of the tone frequency. The DC component is, of course, simply the number of nerve spikes observed; when plotted as a function of stimulus level and properly normalized, this is the rate function. This quantity, as well as the magnitude of the spectral component at the tone frequency, has been studied extensively.

The appearance of these frequency components reveals that the temporal characteristics of tonal stimuli are preserved, in a sort of rectified form, in the fiber discharge pattern. The synchronization index (SI), which represents a measure of the preferential occurrence of neural events over restricted regions of the stimulus phase, is often used. It is defined as the ratio of the spectral component at the tone frequency to that at DC.[3,10–12,23,24] Measurements of the phase of the histogram center, and of the spectral component at the tone frequency, have been discussed in great detail by a number of authors.[2,4,21,28]

In this paper we examine the full spectrum of the period histogram in a systematic way, with particular emphasis on the behavior of the spectral components at harmonics of the tone frequency. We first discuss the responses of units (cells) with low and medium characteristic frequencies (CFs) (and with low and high spontaneous firing rates). We show that only a small number of spectral components are observable and we illustrate how their magnitudes and phases depend on the applied stimulus level for tones that are below, at, and above the CF of the unit.

The responses of high-CF units are discussed subsequently. When the applied tone frequency is also high, the fundamental and harmonic components are substantially attenuated relative to the DC component, so that the SI is reduced. We make use of a specially designed microcomputer-based peak-detection system to measure the times of action-potential occurrences, from which the spectrum of the period histogram is constructed. The results are compared with those obtained by using a conventional level-detection system. This permits us to show that the decrease in the SI at high frequencies arises, at least in part, from uncertainties in the spike occurrence times introduced by noise in the auditory nerve.[37] Finally, the theoretical basis underlying the decrease in the magnitudes of the spectral components in the period histogram is provided.

Period histograms and their spectra for amplitude-modulated (AM) and frequency-modulated (FM) tonal stimuli have been discussed elsewhere.[14,15]

2. METHODS

The VIIIth nerve was exposed in anesthetized cats and extracellular recordings were made from single primary auditory nerve fibers using KCl-filled glass microelectrodes. The criteria used in animal selection, anesthesia, surgical preparation, acoustic-signal generation and measurement, neural-signal recording, and digital-stimulus generation and data analysis have been described previously.[36]

The signal from the microelectrode was amplified with a negative-capacitance amplifier and a preamplifier. In the set of experiments described in Section 3 the output of the preamplifier was applied to a level detector which generated a standard (1 μsec, 10 V) impulse each time the nerve-spike amplitude exceeded a preset adjustable threshold. A period histogram, synchronized to multiple periods of the stimulus, was constructed from a set of these impulses using histogram hardware.[36] The experiments described in Section 4.3 made use of a peak detector (described in Section 4.2) as well as a level detector.

Auditory nerve fibers were identified by using wideband noise-burst

stimuli. Frequency tuning curves (FTCs) were then obtained using the algorithms reported by Kiang *et al.*[18] and by Liberman.[22] The CF of the fiber was determined from the FTC. It was defined as that frequency at which the lowest sound pressure level (SPL) elicited a specified neural response. Two subsidiary frequencies were selected from the FTC, above and below the CF, where the sensitivity was 15 dB below its maximum value at the CF. These frequencies, along with the CF frequency, were then used as the stimulus frequencies in the experiments reported in Section 3.

In the experiments described in Section 3, measurements were first made at the CF. The amplitude of the stimulus was set initially at a level that was either −20 dB:re FTC or at +20 dB:re FTC, depending on the particular experimental paradigm employed. In successive measurements, the stimulus level was increased in 10-dB steps to a maximum value of 70 dB:re FTC. The stimulus in dB:re FTC represents the sound pressure in dB, relative to the sound pressure level of the FTC, at each frequency. The entire series of measurements was then repeated at frequencies below and above the CF.

Period histograms, constructed from the nerve-spike data,[36] usually consisted of 2048 bins, each generally of 25-μsec duration, so that a single pass across the period histogram represented 51.2 msec. In the experiments reported in Section 3, 1000 repetitions of the responses were superimposed to form the histogram, so that data were collected for 51.2 sec at each frequency and level. The maximum values of the spectral magnitude at DC, which represents the total number of spikes in the histogram, at an average spike rate of 100/sec, is therefore $\sim$5000.

The precise values of the frequencies were determined by the computer software so that the total duration of an integral number of cycles of the sinusoidal stimulus exactly fit the duration of the period histogram. Specifying a frequency of 100 Hz, for example, would lead to the selection of a frequency of 97.6 Hz.

Following the averaging, a DFT of the period histogram was constructed, which we refer to as the spectrum. A standard fast-Fourier transform (FFT) algorithm was used in computing the DFT. The data reported in this paper are based on these DFTs.

3. SPECTRAL CHARACTERISTICS FOR LOW AND MEDIUM FREQUENCIES

3.1. Full Spectrum of the Period Histogram

The first experiment involved a high-spontaneous, low-frequency unit with a CF of 625 Hz and a threshold of 23 dB:re SPL. The signal applied

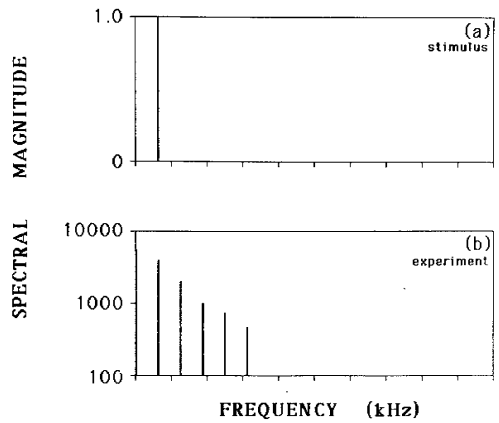

Fig. 1. (a) Spectral magnitude of the signal applied to the ear as a function of frequency. The stimulus is a pure tone of frequency 625 Hz. A single spectral component is seen at the tone frequency. (b) Spectral magnitude of the period histogram as a function of frequency for a high-spontaneous, low-frequency (CF = 625 Hz) unit with a threshold of 23 dB:re SPL. Strong spectral components are seen at DC, at the tone frequency, and at a small number of harmonics of the tone frequency. The magnitudes of the spectral components decrease monotonically as the component frequency increases. The data in (b) are drawn from Fig. 2b at a stimulus level of 20 dB:re FTC.

to the ear was a pure tone of frequency 625 Hz at a level of 20 dB:re FTC; the signal spectrum shown in Fig. 1a therefore consists of a single component at the tone frequency.

The spectral magnitude of the period histogram, as a function of frequency, is illustrated in Fig. 1b. Spectral components are shown only if their magnitudes exceed the average spectral noise floor by 6 dB. Strong spectral components can be seen at DC, at the tone frequency, and at a small number of harmonics of the tone frequency. The highest frequency component that can be seen above the FFT noise floor is at 3125 Hz.

The spectrum of the histogram differs considerably from that of the input. Many new frequency components are present. Spectral-component magnitudes decrease monotonically with increasing component frequency. The character of the spectrum is not unlike that of the velocity response of single outer hair cells and Hensen cells in the guinea-pig temporal-bone preparation.[16,40]

3.2. Behavior of the Spectral Magnitudes with Stimulus Level

The magnitudes of the individual spectral components are shown in Figs. 2a–2c as a function of relative stimulus level (dB:re FTC) for this

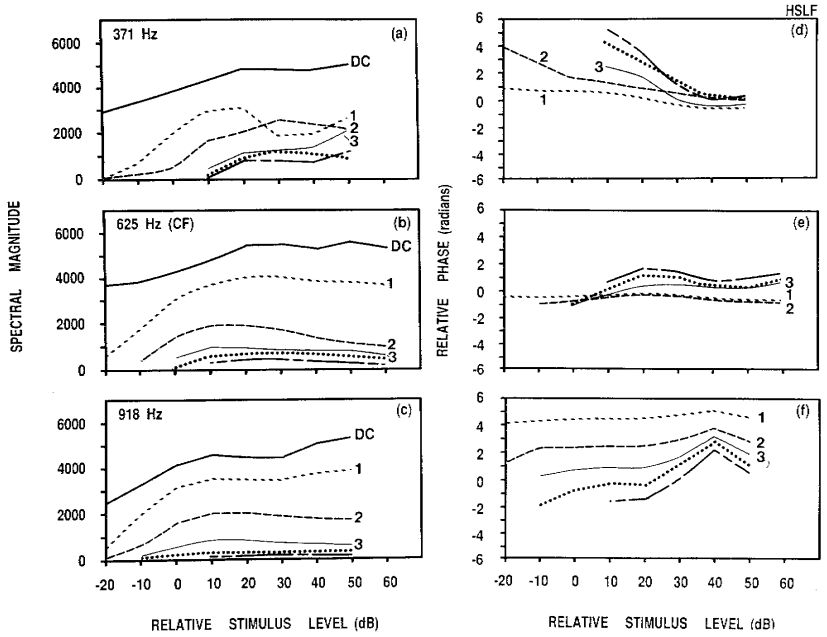

Fig. 2. (a–c) Magnitudes of the spectral components as a function of relative stimulus level (dB:re FTC) for the same unit as shown in Fig. 1, for input frequencies (a) 371 Hz (below CF), (b) 625 Hz (at CF), and (c) 918 Hz (above CF). Curves for DC, for the tone frequency (denoted 1), and for its second through fifth harmonics (denoted 2–5), are shown. (d–f) Relative phases (in radians) of the individual spectral components as a function of stimulus level.

same low-frequency unit. The data in Figs. 2a–2c are for tone frequencies $f_c = 371$ Hz (below CF), 625 Hz (at CF), and 918 Hz (above CF), respectively. The spectral magnitudes at DC, at the tone frequency (denoted 1), and at its second through fifth harmonics (denoted 2–5) are shown as a function of stimulus level for the three frequencies. At any given stimulus level, the magnitudes of the spectral components at DC, the fundamental, and the second, third, fourth, and fifth harmonics successively decrease. Harmonics beyond the fifth are not observable. (The data in Fig. 1b represent a vertical slice drawn from Fig. 2b, at a stimulus level of 20 dB:re FTC.) The only exception is the magnitude of the fundamental component in Fig. 2a, between the levels of 30 and 40 dB. The reason for this unusual behavior is discussed below. All components follow a similar trend in that they increase in magnitude between −20 and 20 dB:re FTC and then either level off or decrease slightly at higher stimulus levels. Above 10 dB:re FTC, their ratios remain roughly the same as the stimulus level is increased.

It is apparent from Figs. 2a–2c that spectral components at the

frequency of the applied tone are usually seen above the FFT noise floor at stimulus levels below the average rate threshold (as determined from the paradigm reported by Kiang *et al.*,[18] which in our case is 0 dB:re FTC. Behavior of this kind was noted by Johnson,[12] who measured a "synchrony tuning curve" with a threshold that was lower by about 20 dB than the rate tuning curve. It is clear from the data presented in Fig. 2 that the emergence of such synchrony applies not only to the spectral component at the tone frequency, but also to the components at harmonics of the tone frequency.

The spectral-component magnitudes for a high-spontaneous, medium-frequency (HSMF) unit, with a threshold of 17 dB:re SPL, are shown in Fig. 3a. The stimulus was a pure tone at 3750 Hz (at the CF) and the stimulus level was varied from −20 to 70 dB:re FTC. The only components that appear in the period-histogram spectrum in this case are at DC, at the tone frequency, and at its second harmonic. The relative phases for these components are shown in Fig. 3b. As the tone and CF frequencies increased from 625 Hz in Fig. 2 to 3750 Hz in Fig. 3, the number of observable AC components decreased from 5 to 2, and the SI decreased as well. This loss of phase locking (also called loss of synchrony) results in part from nerve-spike time jitter, as discussed in Section 5.

The spectral-component magnitudes and relative-phase curves for a low-spontaneous, medium-frequency (LSMF) unit with a threshold of 36

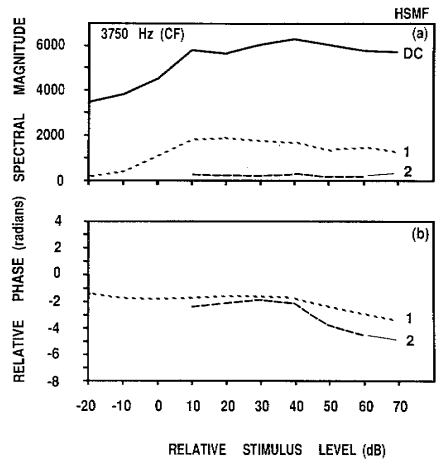

Fig. 3. (a) Magnitudes and (b) relative phases of individual spectral components, as a function of relative stimulus level, for a high-spontaneous, medium-frequency (CF = 3750 Hz) unit, with a threshold of 17 dB:re SPL. The stimulus was at 3750 Hz. Spectral components are seen at DC, at the tone frequency, and at its second harmonic. The SI is lower than that in Fig. 2.

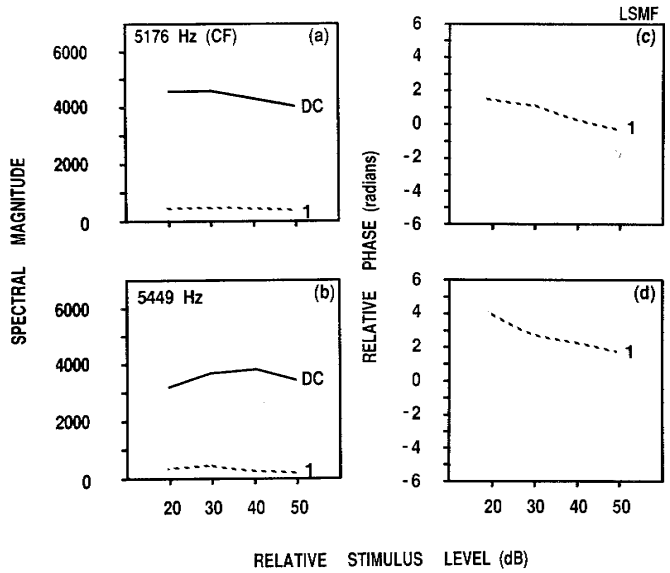

Fig. 4. Magnitudes and relative phases of spectral components at DC and at the tone frequency, as a function of relative stimulus level, for a low-spontaneous, medium-frequency unit (CF = 5176 Hz), with a threshold of 36 dB:re SPL. In (a) and (c), the stimulus was at 5176 Hz. Only one AC component (at the tone frequency) emerges above the noise and the SI is lower still than that in Fig. 3. In (b) and (d) the stimulus frequency was at 5449 Hz, above the CF.

dB:re SPL are presented in Figs. 4a and 4b. Figures 4a and 4c show the magnitude and the phase response to a tone at $f_c = 5176$ Hz (at the CF), applied at levels between 20 and 50 dB:re FTC. Responses at 5449 Hz (above the CF) are shown in Figs. 4b and 4d. Spectral components are seen only at DC and at the tone frequency itself and the SI is yet lower than that observed in Fig. 3.

The variation of the spectral magnitudes follows certain patterns:

(i) The number of harmonics observed in the spectrum of the period histogram is small. It depends on the stimulus frequency (and the CF of the unit). For example, four harmonics are seen at a CF of 625 Hz (Fig. 2), one at a CF of 3750 Hz (Fig. 3), and none at a CF of 5176 Hz (Fig. 4). In general the higher the stimulus frequency, the fewer the number of harmonics present. The limited number of harmonics, and their decrease in magnitude with increasing frequency, arises from two effects, as discussed in Sections 4 and 5.

(ii) At any given stimulus level, the spectral-component magnitudes decrease monotonically as the harmonic number increases. Both even and

odd harmonics are present. (A spectrum of this kind is most simply generated by asymmetrically clipping a sinewave; see ref. 38.) There are a few special conditions under which the spectral-component magnitudes do not decrease monotonically with harmonic number, such as low-CF units stimulated by low-frequency tones. For example, the magnitude of the fundamental component is smaller than that of the second harmonic in Fig. 2a for stimulus levels between 30 and 40 dB:re FTC. This behavior is associated with peak splitting in the period histogram.[12] It occurs because under these conditions two neural spikes can occur during the same half cycle of the stimulus waveform.

(iii) For a stimulus at a given frequency and at a level above the average rate threshold (0 dB:re FTC), the spectral magnitudes of the different frequency components bear a general proportionality to each other (and to the DC component) as the stimulus level changes. The relative proportions of the various spectral components turn out to be reasonably constant over some 50 dB change in stimulus level. This suggests that the shape of the underlying rectified wave remains essentially unchanged with stimulus level over this intensity range.

(iv) The spectral magnitudes of the highest harmonics are generally stronger below CF than above CF (compare Figs. 2a and 2c).

3.3. Behavior of the Relative Phases with Stimulus Level

The relative unwrapped phases of the individual spectral components are illustrated in Figs. 2d–2f, 3b, 4c, and 4d as a function of stimulus level. Below CF at a stimulus level of 10 dB:re FTC, in Fig. 2d, the phase angle increases in the sequence: fundamental, second, third, fourth, and fifth harmonics. The phase angle is roughly proportional to the harmonic number (which is consistent with constant delay). Therefore the slope of the phase, with respect to harmonic number, is positive. The phase difference between successive harmonics decreases as stimulus level is increased. The phase versus intensity curve has a negative slope. In this region, there is not an orderly arrangement of phase as a function of harmonic number.

At CF, in Fig. 2e, the phase curves do not form an orderly sequence with harmonic number because the phase angles are small. The phases of the individual components are roughly independent of level.

Above CF, in Fig. 2f, the phase angles decrease with increasing harmonic number. The phase difference between the fundamental and a given harmonic is proportional to harmonic number. Therefore the slope of the phase with respect to harmonic number is negative. The phase differences between the components decrease as stimulus level is increased, up to

40 dB:re FTC. The slope of the phase versus intensity curve is positive in this region. The downturn of the phase curves above 40 dB probably arises from ambiguity in unwrapping the phase.

These observations are consistent with the findings of earlier investigators who measured phase as a function of frequency.[2,4] When the frequency was below CF, the phase slope (with respect to frequency) was positive; near CF the phase slope was small or zero; and above CF the phase slope was negative. The phase slopes decreased as stimulus intensity was increased.

4. LOSS OF SYNCHRONY AT HIGH FREQUENCIES: PEAK VERSUS LEVEL DETECTION

It is apparent from the foregoing that the fundamental and harmonic components in the period histogram diminish as the stimulus frequency increases. Indeed, stimuli above about 6 kHz are generally assumed to elicit only a DC component in the period histogram.[11,12,29] Spectral components well above 6 kHz can be present, however. Inaccuracies in the determination of nerve-spike occurrence times, associated with cochlear-nerve noise and level-detection measurement techniques, are in part responsible for the apparent loss of these high-frequency components.[37] The use of peak-detection nerve-spike measurement techniques can enhance the observability of such high-frequency components.

4.1. Effect of Background Noise on Level and Peak Detection

The classical method of recording auditory nerve spikes makes use of a microelectrode whose output is fed into a high-input-impedance, negative-capacitance feedback amplifier.[17] This serves to compensate for the microelectrode capacitance, thereby improving the frequency response of the detection system. The frequency response of the negative-capacitance amplifier depends on the feedback control setting, which is adjustable. The real nerve-spike risetime and shape are therefore altered by the electrode/feedback-amplifier combination. The signal is generally further amplified and then applied to a Schmitt trigger, which produces a standard timing pulse at the instant its input voltage exceeds a preset adjustable threshold.[9] The threshold is set at a level below the peak of the nerve spikes but above the noise floor. The sequence of nerve spikes is thus converted into a sequence of standard electrical pulses on which further analyses are carried out.

The occurrence times registered by the electrical pulses are affected by the presence of background noise in the auditory nerve as a whole. It

is therefore important to understand the character of this noise. Measurements were made of the distribution in frequency of the baseline noise, employing the same microelectrode and amplifier used for nerve-spike recording. The distinction was that the electrode was not in close contact with an auditory nerve fiber and therefore was not recording nerve-spike potentials. The compensation of the negative-capacitance feedback amplifier was set at a minimum for these measurements so that the frequency response was essentially determined by the electrode. A typical result at the output of the negative-capacitance amplifier is illustrated in Fig. 5. The noise voltage is highest at low frequencies and decreases in power-law fashion, over a substantial range of frequencies, as the frequency increases.

The way that such low-frequency noise can contaminate the determination of nerve-spike occurrence times is illustrated in Fig. 6. The height of the nerve impulse relative to the threshold level of the Schmitt trigger in the level-detection system (dashed horizontal line) will vary as a result of the presence of low-frequency noise fluctuations (two realizations are shown, as the upper and lower schematic nerve impulses). Because of the finite risetime of the amplified and filtered action potential, the level-detection timing pulse shown at A will be produced earlier or later, depending on whether the instantaneous noise amplitude is high or low. The magnitude of the uncertainty (jitter) Δt will depend both on the character

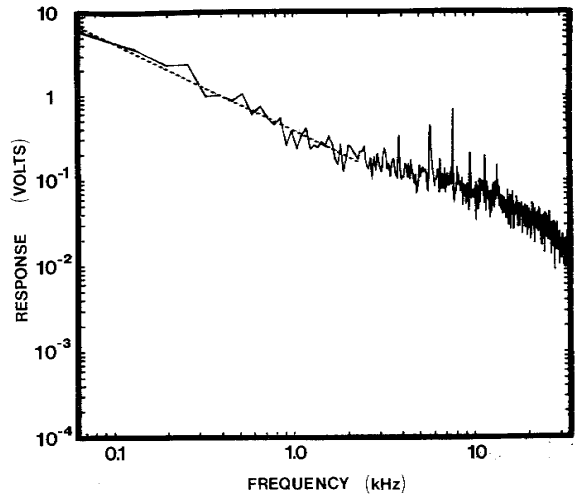

Fig. 5. Voltage versus frequency for background noise in the auditory nerve as observed through the microelectrode/feedback-amplifier system. The magnitude decreases in power-law fashion over a substantial frequency range.

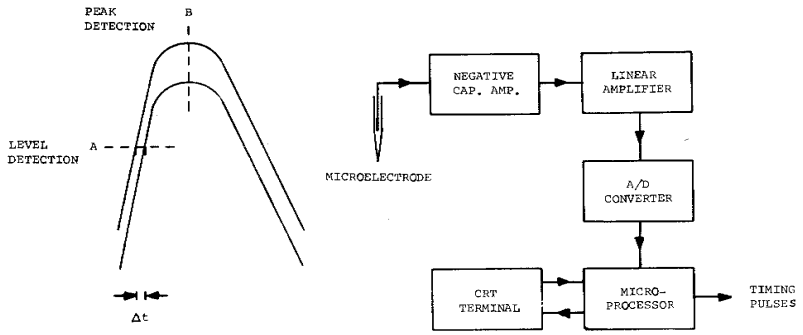

Fig. 6. Schematic representation of a nerve spike in two vertical positions. The upper and lower curves correspond to a hypothetical peak and dip, respectively, in the low-frequency auditory-nerve noise. The level-detection system (A) introduces a random time uncertainty Δt in the timing pulse that is dependent on the instantaneous level of the noise and on the rising slope of the filtered nerve spike. The peak-detection system (B), on the other hand, introduces no such time uncertainty. A block diagram of the system incorporating the specially constructed peak-detection microprocessor is shown on the right.

of the noise and on the rising slope of the action potential. Typically, $\Delta t \approx 100$ μsec. It is evident at B, however, that the timing of the peak of the filtered action potential (dashed vertical line) is affected less by the presence of such low-frequency noise. This is because the nerve spike rides up and down vertically as the baseline fluctuates. Using a peak-detection mechanism, rather than a level-crossing detection mechanism, should therefore minimize time jitter arising from power-law auditory-nerve noise.

4.2. Microcomputer-Based Peak-Detection System

A special microcomputer was developed to generate electrical timing pulses coincident with the peaks of the nerve spikes; a block diagram is shown on the right-hand side of Fig. 6. The output of the negative-capacitance amplifier is passed through a linear amplifier (to provide a peak voltage of about 5 V) and then sampled by an analog-to-digital (A/D) converter. A digital sample is processed every 18 μsec by an Intel 8085 microprocessor to determine when the input waveform exceeds a present value (2.5 V). This defines the presence of a nerve spike. Subsequent samples are successively compared in real time to identify the occurrence time of the peak. When the peak sample is identified, the microprocessor outputs a timing pulse and immediately returns to sampling the nerve-spike signal to determine when the trailing edge of the spike falls below 0.625 V. At that point, the microcomputer begins again to collect samples to detect the presence of the next nerve spike.

Experiments were carried out to measure the spectrum of the period

histogram and the SI using this peak-detection apparatus. For comparison, identical measurements were also made using the classical level-detection technique.

4.3. Comparison of Synchronization Index Using Peak and Level Detection

The stimuli were all pure tones. The general experimental methods and parameters are the same as those outlined in Section 2, with a few minor exceptions. Bin widths ranged from 15 to 25 μsec and typical averaging times ranged from 30 to 50 sec for 200–1000 identical repetitions of the stimulus. The results reported in this section were based on experiments with 10 cats.

At low frequencies we determined that the spectrum of the period

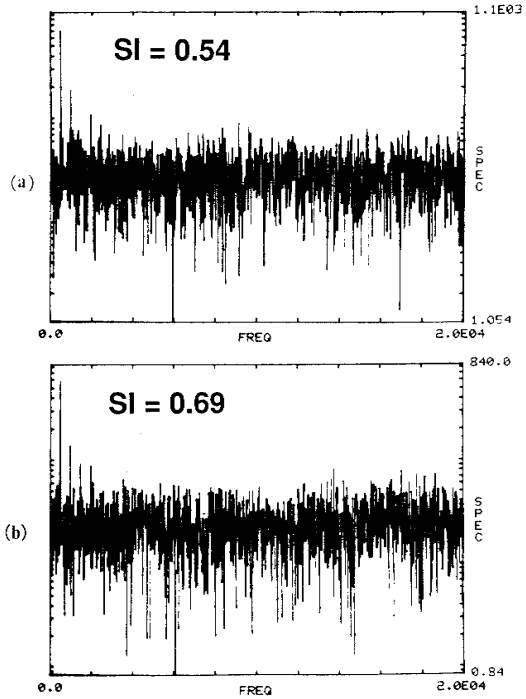

Fig. 7. Spectral magnitude of the period histogram (200 repetitions) as a function of frequency for a low-frequency unit with characteristic frequency CF = 488 Hz. The unit was stimulated with a pure tone of level 80 dB re SPL at the CF. (a) Result using the conventional level-detection system. (b) Result using the peak-detection system. The SI observed with the peak-detection system (0.69) is only slightly greater than that observed with the level-detection system (0.54). The spectral components in both are similar, diminishing substantially beyond about $4f_c \approx 2$ kHz.

histogram and the SI obtained from experiments conducted with peak and level detectors were comparable. This is illustrated in Fig. 7 for a unit driven with a pure-tone stimulus at its CF (488 Hz). The spectral components in both are similar, diminishing substantially beyond the fourth harmonic at $4f_c \approx 2$ kHz. The results for both detection schemes are not unlike those shown in Fig. 1, where the CF is 625 Hz.

Differences in the values of the SI using the two techniques begin to emerge at about 5 kHz and become quite pronounced above 10 kHz. A comparison of several experimentally measured values of the SI using the two methods is presented in Table I. The SI for each of the four units stimulated at 10 kHz or above is higher using the peak detector. Indeed, the absolute values of the SI are substantial even at a frequency as high as 10 kHz. In Fig. 8, we present the spectrum for Unit No. 10 using level and peak detection, represented in Figs. 8a and 8b, respectively. The two sets of data were collected under identical conditions. The substantially larger value of the SI observed with the peak-detection apparatus is evident.

The highest frequency at which we have observed substantial phase locking (synchrony) is 18 kHz. In fact, Rose *et al.*[29] long ago observed signs of phase locking at frequencies as high as 12 kHz in isolated instances (in squirrel monkeys). They suggested that the observation of synchrony could depend on measurement timing accuracy. Johnson[12] carried out a series of experiments (on cats) in which he observed synchrony only up to 6 kHz. He also carried out a theoretical analysis[11] demonstrating that this limit was not attributable to instrumental effects. More recently, Sullivan and Konishi[32] showed that phase locking in the magnocellular cochlear nucleus of the barn owl extends to 9 kHz, but they considered the presence of a measurable SI at 9 kHz as a special characteristic of the barn owl. Sullivan and Konishi also used both level and peak detection, but they saw little difference in the values of the SI.

Table I. Comparison of Synchronization Index (SI) When Spike Occurrence Times Were Measured with Peak and Level Detectors

Unit No.	CF and tone frequency (Hz)	Approximate dB SPL (re 0.0002 dyne/cm^2)	Number of averages N	SI using peak detector	SI using level detector
12	10,742	60	6000	0.03	0.001
10	10,000	100	1000	0.31	0.10
28	11,992	100	1000	0.27	0.06
38	5,501	100	1000	0.09	0.09
45	11,002	100	2000	0.10	0.07

The large values of the SI that we observed at these high frequencies might, at first blush, be thought to arise from substantial averaging (the SI is generally assumed to increase as the number of averages is increased). We conducted several experiments to investigate whether this is the case. The results of two such experiments are shown in Table II. In one experiment, on a unit with a CF of 15,996 Hz, the SI did not change substantially as the number of averages was reduced; if anything, it appeared to increase slowly. In another experiment, with a unit whose CF was 10,000 Hz, the SI also increased as the number of averages was reduced from 200 to 3. Although we noted some nonmonotonicity in the SI versus number-of-averages function, it is clear that the large values of the SI at these high frequencies are not an artifact of excessive averaging.

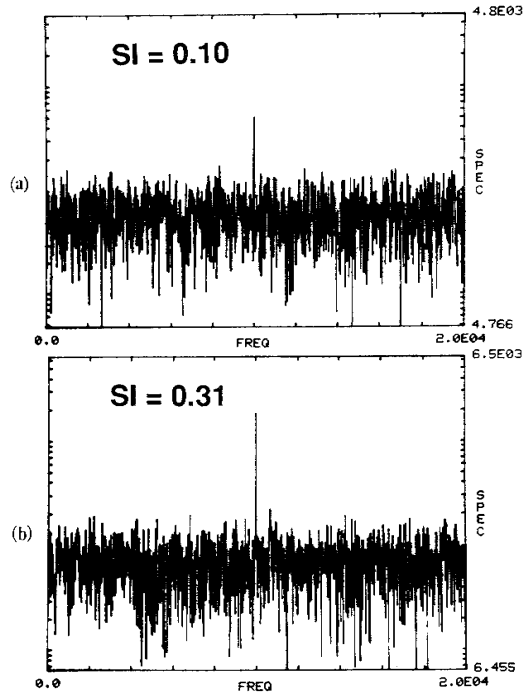

Fig. 8. Spectral magnitude of the period histogram (collected with 1000 repetitions) as a function of frequency for a high-frequency unit (#10) with a CF = 10 kHz. The unit was stimulated with a pure tone of level 100 dB:re SPL at the CF. (a) Result using the conventional level-detection system. (b) Result using the peak-detection system. As shown in Table I, the SI obtained from the spectral component at 10 kHz with the peak-detection system (0.31) is substantially greater than that observed with the level-detection system (0.10). These results show clearly that phase locking extends to at least 10 kHz.

Table II. Behavior of SI Using Peak Detector As the Number of Averages *N* Decreases

Unit No.	CF and tone frequency (Hz)	Approximate dB SPL (re 0.0002 dyne/cm^2)	Number of averages N	SI using peak detector
33	15,996	100	2000	0.06
			1000	0.10
			500	0.09
			100	0.16
10	10,000	100	1000	0.31
			200	0.41
			50	0.51
			10	0.46
			5	0.50
			3	0.60

Finally, we briefly examine the dependence of the SI on the frequency response of the microelectrode and its associated amplifier system. These elements should partially determine the risetime of the recorded action potential and therefore would be expected to play a role in the magnitude of the time jitter. To maximize the frequency response, glass microelectrodes with resistances in the 5- to 10-MΩ range were utilized. The overall frequency response of our recording system can be changed by varying the cutoff frequencies of the linear amplifier and by adjusting the negative-capacitance feedback control (see Fig. 6). The results of these two manipulations are illustrated in Table III. As the upper frequency cutoff of

Table III. Effect of Analog Signal Processing on the SI[a]

Unit No.	CF and tone frequency (Hz)	Approximate dB SPL (re 0.0002 dyne/cm^2)	Number of averages N	Amp f_{max} (kHz)	Neg. cap. comp.	SI using peak detector
10	10,000	100	1000	3	—	0.44
				10	—	0.49
				10	Min	0.29
				10	Max	0.52

[a] The column labeled Amp f_{max} indicates the upper frequency cutoff of the linear amplifier. The column labeled Neg. cap. comp. indicates minimum or maximum negative-capacitance compensation.

the linear amplifier is increased from 3 kHz to 10 kHz, the SI for Unit No. 10 increases only slightly (from 0.44 to 0.49). The increase is more pronounced when the negative-capacitance compensation is adjusted from minimum (SI = 0.29) to maximum (SI = 0.52). These results indicate that even with peak detection, an increase in the frequency response of the system improves the timing information and therefore the synchronization index. A system with higher frequency response will follow the nerve action potentials more faithfully and therefore define their times more precisely. At present, the upper frequency limit at which synchrony may be observed with our apparatus is limited by the frequency response of the microelectrode/amplifier system and by the time resolution of the microcomputer and histogram hardware.

In short, we have demonstrated that neural spike trains in cat auditory fibers are capable of carrying high-frequency timing information.

5. THEORETICAL BASIS FOR THE BEHAVIOR OF THE PERIOD-HISTOGRAM SPECTRUM

We have seen that the spectrum of the period histogram recorded from primary auditory-nerve fibers stimulated by pure tones contains components at DC, at the applied tone frequency, and at a small number of harmonics. The magnitudes of the spectral components generally decrease as the frequency increases.

In this section, we examine the basis of this behavior from a theoretical point of view. This enables us to understand the manner in which stimulus frequency, and uncertainties in the measurement of nerve-spike occurrence times, affect the magnitudes of the spectral components and the synchronization index.

There are two origins of the decrease in spectral-component magnitudes with increasing frequency. The first, operative for pure-tone stimuli at low frequencies, arises from the time uncertainty associated with the distribution of neural events within a half-cycle of the stimulus waveform. A graphical illustration of this is provided in Fig. 9. A half-wave-rectified sinusoidal time signal $s(t)$ is assumed to represent the period histogram, but this choice of waveform is convenient, not critical. The same argument will carry through for a more realistic waveform, such as that obtained from a nonlinear-stiffness oscillator model (see, e.g., ref. 39). (Indeed, the same approach can be used for arbitrary periodic waveforms, such as those arising from superpositions of two or more tones.) The signal $s(t)$ can be mathematically represented as a convolution (for which we use the symbol $*$) of three functions: a perfect train of delta functions spaced by the period of the stimulus tone T, a pulse (of full width $T/2$)

representing a single half-cycle of the stimulus, and a pulse of half-width τ_p representing the uncertainty in the nerve-spike measurement time (τ_p will depend on the method used for nerve-spike measurement).

Since convolution in the time domain corresponds to multiplication in the frequency domain, the spectrum $S(f)$ can be represented as a product of the Fourier transforms of each of the three functions indicated above: a perfect train of delta functions at the frequency of the stimulus tone $f_c = 1/T$, a function of approximate width $4f_c$ corresponding to the

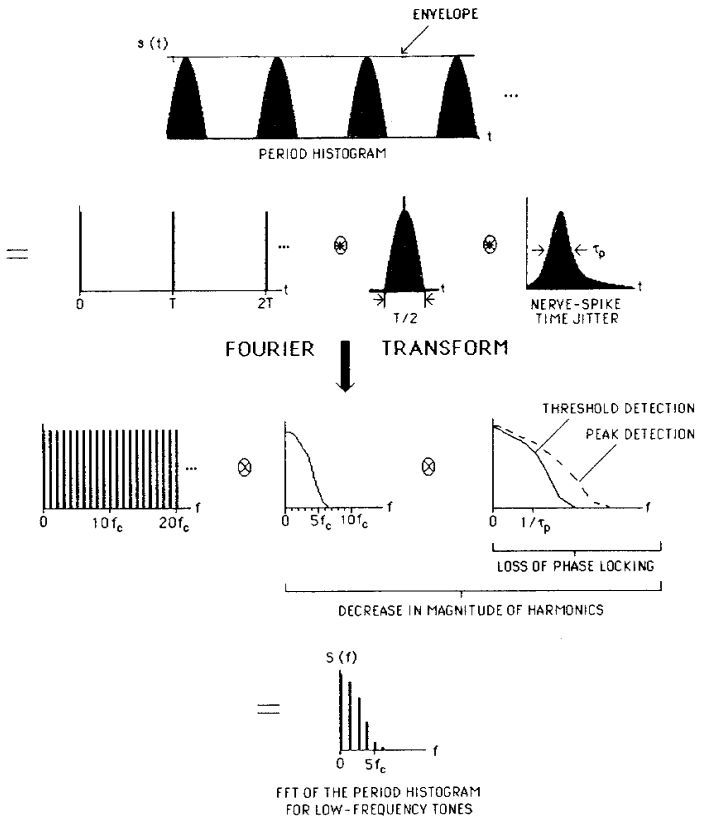

Fig. 9. Graphical derivation of the spectrum of the period histogram for low-frequency pure-tone signals. The overall decrease in the magnitudes of the spectral components with increasing frequency is caused principally by the uncertainty in the time of neural-event occurrences within the half-wave-rectified period histogram. The lower the stimulus frequency, the greater this time uncertainty and the lower the frequency at which the spectral components begin to diminish. There is minimal loss of phase locking when the characteristic cutoff frequency caused by nerve-spike jitter is larger than $4f_c$.

frequency bandwidth of a half cycle of the stimulus, and a function of approximate width $1/\tau_p$ representing the frequency bandwidth of the nerve-spike time jitter.

The decrease in the magnitude of the harmonics is seen to be governed in Fig. 9 principally by the large uncertainty in the time of nerve-spike occurrences within a half-cycle of the stimulus. The lower the stimulus frequency, the greater this time uncertainty and the lower the frequency at which the spectral components begin to diminish (they extend to about $4f_c$). A numerical example is instructive: if $f_c = 500$ Hz and $\tau_p \approx 0.2$ msec, then $1/\tau_p = 5$ kHz, which is $> 4f_c = 2$ kHz, so that the nerve-spike time jitter is not important in this case. Although all of the harmonics are at relatively low frequencies, the SI remains high. The data shown in Fig. 1, for which $f_c = 625$ Hz and SI ≈ 0.65, behave in this way. A simple half-wave rectifier model gives a synchronization index SI $= \pi/4 \approx 0.79$.

Since nerve-spike jitter does not critically affect the harmonic components for low frequencies, there is minimal loss of phase locking and the observed spectrum should depend little on whether threshold detection or peak detection is used. Both should give essentially the same results, and they do. These predictions are borne out by the experimental results shown in Fig. 7, in which the spectrum and SI observed with the peak-detection system (0.69) closely resemble those observed with the level-detection system (0.54). The spectral components in both diminish below detectability beyond a frequency of about $4f_c \approx 2$ kHz.

The second origin of the decrease of spectral-component magnitudes is operative for stimuli of high frequencies. It arises, at least in part, from temporal uncertainties in the spike occurrence times. As shown in Fig. 6, these can be introduced by level detection in the presence of auditory-nerve background noise. A graphical illustration of this case is presented in Fig. 10. The resultant loss of phase locking causes the SI, and in fact the magnitudes of all of the harmonic components, to decrease when the tone frequency is greater than the inverse jitter time $1/\tau_p$. The jitter rolloff is independent of the stimulus frequency. Again a numerical example is instructive; if $\tau_p \approx 0.2$ msec, then $1/\tau_p = 5$ kHz, which is the limit beyond which phase locking will diminish substantially, whatever the stimulus frequency. In this region, a simple half-wave rectifier model gives SI $= (\pi/4)\,|H(f_c)|/|H(0)| < 0.79$, where $H(f)$ is the Fourier transform of the nerve-spike time-jitter function.

At these high frequencies, a greater degree of phase locking should be achievable by using peak detection (which serves to decrease the jitter time τ_p, thereby increasing $1/\tau_p$) rather than level detection. This is in fact precisely what happens, as is evident in Fig. 8. As indicated above, we have observed substantial phase locking at tone frequencies as high as 18 kHz

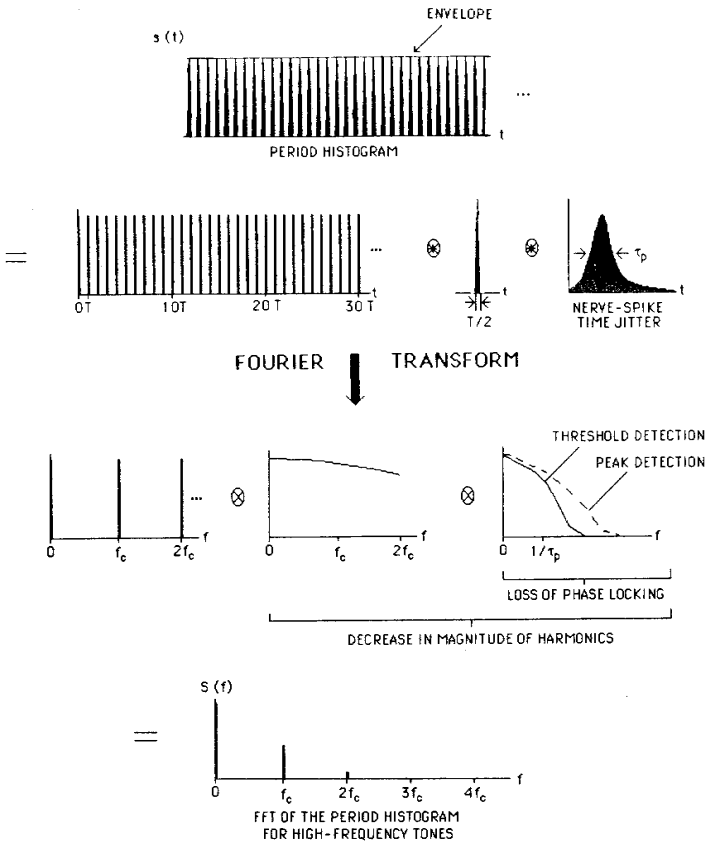

Fig. 10. Graphical derivation of the spectrum of the period histogram for high-frequency pure-tone signals. The overall decrease in the magnitudes of the spectral components with increasing frequency is caused principally by the frequency rolloff associated with nerve-spike time jitter. There is substantial loss of phase locking when this characteristic cutoff frequency $(1/\tau_p)$ is smaller than f_c. The phase locking can be extended by using peak detection rather than level detection. For clarity, the function $s(t)$ is shown without the effect of nerve-spike time jitter.

using peak detection. We conclude that the traditional view, that there is an intrinsic loss of phase locking for tone frequencies above 6 kHz, is in error. This result is important because it indicates that the place-versus-periodicity dichotomy in auditory theory should be reexamined.

ACKNOWLEDGMENTS

This work was supported by the Office of Naval Research under Grant No. N00014-92-J-1251, by the National Institutes of Health under NIDCD Program Project Grant DC-00316, and by the Emil Capita Foundation.

REFERENCES

1. M. Abeles, Quantification, smoothing, and confidence limits for single-units' histograms, *J. Neurosci. Meth.* **5**:317–325 (1982).
2. J. B. Allen, Magnitude and phase-frequency response to single tones in the auditory nerve, *J. Acoust. Soc. Am.* **73**:2071–2092 (1983).
3. D. J. Anderson, Quantitative model for the effects of stimulus frequency on synchronization of auditory nerve discharges, *J. Acoust. Soc. Am.* **54**:361–364 (1973).
4. D. J. Anderson, J. E. Rose, J. E. Hind, and J. F. Brugge, Temporal position of discharges in single auditory nerve fibers within the cycle of a sine-wave stimulus: Frequency and intensity effects, *J. Acoust. Soc. Am.* **49**:1131–1139 (1971).
5. E. F. Evans, The frequency response and other properties of single fibers in the guinea-pig cochlear nerve, *J. Physiol.* (London) **226**:263–287 (1972).
6. E. F. Evans, Cochlear nerve and cochlear nucleus, in *Handbook of Sensory Physiology*, Vol. V/2, *Auditory System*, W. D. Keidel and W. D. Neff, eds. (Springer-Verlag, Berlin, 1975), pp. 1–108.
7. R. Galambos and H. Davis, The response of single auditory-nerve fibers to acoustic stimulation, *J. Neurophysiol.* **6**:39–57 (1943).
8. G. L. Gerstein and N. Y.-S. Kiang, An approach to the quantitative analysis of electrophysiological data from single neurons, *Biophys. J.* **1**:15–28 (1960).
9. E. Glaser and D. J. Ruchkin, *Principles of Neurobiological Signal Analysis* (Academic Press, New York, 1976), pp. 291–371.
10. J. M. Goldberg and P. B. Brown, Response of binaural neurons of dog superior olivary complex to dichotic tonal stimuli: Some physiological mechanisms of sound localization, *J. Neurophysiol.* **32**:613–636 (1969).
11. D. H. Johnson, The relationship of post-stimulus time and interval histograms to the timing characteristics of spike trains, *Biophys. J.* **22**:413–430 (1978).
12. D. H. Johnson, The relationship between spike rate and synchrony in response of auditory-nerve fibers to single tones, *J. Acoust. Soc. Am.* **68**:1115–1122 (1980).
13. Y. Katsuki, T, Sumi, H. Uchiyama, and T. Watanabe, Electric responses of auditory neurones in cat to sound stimulation, *J. Neurophysiol.* **21**:569–588 (1958).
14. S. M. Khanna and M. C. Teich, Spectral characteristics of the responses of primary auditory-nerve fibers to amplitude-modulated signals, *Hearing Res.* **39**:143–158 (1989).
15. S. M. Khanna and M. C. Teich, Spectral characteristics of the responses of primary auditory-nerve fibers to frequency-modulated signals, *Hearing Res.* **39**:159–176 (1989).
16. S. M. Khanna, M. Ulfendahl, and Å. Flock, Waveforms and spectra of cellular vibrations in the organ of Corti, *Acta Otolaryngol. Suppl.* (Stockholm) **467**:189–193 (1989).
17. N. Y.-S. Kiang, Peripheral neural processing of auditory information, in *Handbook of Physiology: The Nervous System*, Vol. 3, *Sensory Processes*, I. Darian Smith, ed. (American Physiological Society, Bethesda, Maryland, 1984), pp. 639–674.
18. N. Y.-S. Kiang, E. C. Moxon, and R. A. Levine, Auditory-nerve activity in cats with normal and abnormal cochleas, in *Sensorineural Hearing Los*, G. E. W. Wolstenholme and J. Knight, eds. (Churchill, London, 1970), pp. 241–273.

19. N. Y.-S. Kiang, T. Watanabe, E. C. Thomas, and L. F. Clark, Stimulus coding in the cat's auditory nerve, *Ann. Otol. Rhinol. Laryngol.* **71**:1009–1026 (1962).
20. N. Y.-S. Kiang, T. Watanabe, E. C. Thomas, and L. F. Clark, *Discharge Patterns of Single Fibers in the Cat's Auditory Nerve* (MIT Press, Cambridge, Massachusetts, 1965).
21. D. O. Kim, C. E. Molnar, and J. W. Matthews, Cochlear mechanics: Nonlinear behavior in two-tone responses as reflected in cochlear-nerve-fiber responses and in ear-canal sound pressure, *J. Acoust. Soc. Am.* **67**:1704–1721 (1980).
22. M. C. Liberman, Auditory-nerve response from cats raised in a low-noise chamber, *J. Acoust. Soc. Am.* **63**:442–455 (1978).
23. W. M. Littlefield, Investigation of the linear-range of the peripheral auditory system, Sc.D. thesis, Washington University (1973) (Available from University Microfilms, Ann Arbor, Michigan, No. 74-13808).
24. W. M. Littlefield, R. R. Pfeiffer, and C. E. Molnar, Modulation index as a response criterion for discharge activity, *J. Acoust. Soc. Am.* **51**:93 (1972).
25. A. Longtin, A. Bulsara, and F. Moss, Time-interval sequences in bistable systems and the noise-induced transmission of information by sensory neurons, *Phys. Rev. Lett.* **67**:656–659 (1991).
26. S. B. Lowen and M. C. Teich, Doubly stochastic Poisson point process driven by fractal shot noise, *Phys. Rev. A* **43**:4192–4215 (1991).
27. S. B. Lowen and M. C. Teich, Auditory-nerve action potentials form a nonrenewal point process over short as well as long time scales, *J. Acoust. Soc. Am.* **92**:803–806 (1992).
28. R. R. Pfeiffer and C. E. Molnar, Cochlear nerve fiber discharge patterns: Relationship to the cochlear microphonic, *Science* **167**:1614–1616 (1970).
29. J. E. Rose, J. F. Brugge, D. J. Anderson, and J. E. Hind, Phase-locked response to low-frequency tones in single auditory nerve fibers of the squirrel monkey, *J. Neurophysiol.* **30**:769–793 (1967).
30. J. E. Rose, J. F. Brugge, D. J. Anderson, and J. E. Hind, Patterns of activity in single auditory nerve fibers of the squirrel monkey, in *Hearing Mechanisms in Vertebrates*, A. V. S. deReuck and J. Knight, eds. (Little Brown, Boston, Massachusetts, 1968), pp. 144–157.
31. J. E. Rose, J. E. Hind, D. J. Anderson, and J. F. Brugge, Some effects of stimulus intensity on response of auditory nerve fibers in the squirrel monkey, *J. Neurophysiol.* **34**:685–699 (1971).
32. W. E. Sullivan and M. Konishi, Segregation of stimulus phase and intensity coding in the cochlear nucleus of the barn owl, *J. Neurosci.* **4**:1787–1799 (1984).
33. I. Tasaki, Nerve impulses in individual auditory nerve fibers of guinea pig, *J. Neurophysiol.* **17**:97–122 (1954).
34. M. C. Teich, Fractal character of the auditory neural spike train, *IEEE Trans. Biomed. Eng.* **36**:150–160 (1989).
35. M. C. Teich, Fractal neuronal firing patterns, in *Single Neuron Computation*, T. McKenna, J. Davis, and S. F. Zornetzer, eds. (Academic Press, Boston, Massachusetts, 1992), Chapter 22, pp. 589–625.
36. M. C. Teich and S. M. Khanna, Pulse-number distribution for the neural spike train in the cat's auditory nerve, *J. Acoust. Soc. Am.* **77**:1110–1128 (1985).
37. M. C. Teich and S. M. Khanna, Loss of synchrony in auditory nerve fibers, in *Abstracts of the Twelfth Midwinter Research Meeting of the Association for Research in Otolaryngology, Feb. 5–9, 1989*, Abstract No. 138, p. 122.
38. M. C. Teich, S. E. Keilson, and S. M. Khanna, Rectification models in cochlear transduction, *Acta Otolaryngol. Suppl.* (Stockholm) **467**:235–240 (1989).
39. M. C. Teich, S. E. Keilson, and S. M. Khanna, Models of nonlinear vibration. II. Oscillator with bilinear stiffness, *Acta Otolaryngol. Suppl.* (Stockholm) **467**:249–256 (1989).
40. M. C. Teich, S. M. Khanna, and S. E. Keilson, Nonlinear dynamics of cellular vibrations in the organ of Corti, *Acta Otolaryngol. Suppl.* (Stockholm) **467**:265–279 (1989).
41. M. C. Teich, R. G. Turcott, and S. B. Lowen, The fractal doubly stochastic Poisson point process as a model for the cochlear neural spike train, in *The Mechanics and Biophysics of Hearing*, P. Dallos, C. D. Geisler, J. W. Matthews, M. A. Ruggero, and C. R. Steele, eds. (Springer-Verlag, New York, 1990), pp. 354–361.
42. M. C. Teich, D. H. Johnson, A. R. Kumar, and R. G. Turcott, Rate fluctuations and fractional power-law noise recorded from cells in the lower auditory pathway of the cat, *Hearing Res.* **46**:41–52 (1990).

Printed by Catherine Press, Ltd., Tempelhof 41, B-8000 Brugge, Belgium